NATIONAL ADVISORY COMMITTEE FOR AERONAUTICS

TECHNICAL NOTE 3499

CALCULATION OF THE SUPERSONIC PRESSURE DISTRIBUTION ON A SINGLE-CURVED TAPERED WING IN REGIONS NOT INFLUENCED BY THE ROOT OR TIP

By Walter G. Vincenti and Newman H. Fisher, Jr.

Ames Aeronautical Laboratory
Moffett Field, Calif.

Washington
June 1955

LB

NATIONAL ADVISORY COMMITTEE FOR AERONAUTI(

TECHNICAL NOTE 3499

CALCULATION OF THE SUPERSONIC PRESSURE DISTRIBUTION ON A SINGLE-CURVED TAPERED WING IN REGIONS NOT INFLUENCED BY THE ROOT OR TIP

By Walter G. Vincenti and Newman H. Fisher, Jr.

SUMMARY

The shock-expansion method for the calculation of the pressure distribution on cylindrical wings in supersonic flow is here extended to tapered wings made up of single-curved (i.e., developable) surfaces. The method applies in regions of the wing where (a) the component of velocity normal to the surface rulings is supersonic and (b) the flow is not influenced by the presence of the root or tip. The calculation is carried out by regarding the single-curved surface as the limit of an inscribed polyhedron whose edges coincide with rulings of the actual surface. The changes of flow across an element consisting of an edge and subsequent face of the polyhedron are then found from elementary considerations of infinitesimal plane waves and simple geometry. The result, in the limit of the curved surface, is a pair of simultaneous, nonlinear ordinary differential equations for the components of Mach number normal and tangential to the surface rulings. These equations are readily integrated by standard numerical methods in any given case. Calculations are carried through in the present report for a biconvex triangular wing of aspect ratio 4 at two values of the free-stream Mach number.

As usual, the small-disturbance assumptions can be used to provide considerable simplification. In the linear case, in particular, a closed expression is readily obtained for the pressure distribution on a wing of biconvex section. For the calculated example, the relationship between the linear and the shock-expansion results is similar to that observed in two-dimensional flow. In the hypersonic case it is found that the pressure distribution can be calculated by disregarding the taper and treating the streamwise section from a simple two-dimensional point of view. Examination of two-dimensional shock-expansion results for the calculated example shows, in fact, that a strip approximation of this kind provides good accuracy even at moderate supersonic Mach numbers.

INTRODUCTION

The present report is concerned with a type of inviscid supersonic flow that occurs on tapered wings made up of single-curved surfaces. By

"single-curved" it is meant that the surfaces are capable of being developed onto a plane. Such developable surfaces fall into three classes: cylinders, cones, and convolutes, the last being the relatively uncommon surface generated by a straight line moving tangent to a nonplanar curve (see, e.g., refs. 1 and 2). The supersonic flow over an infinite cylinder, yawed or unyawed, can be treated by the two-dimensional shock-expansion method, first proposed by Epstein (ref. 3) and since discussed in numerous books and papers (see, e.g., refs. 4 and 5). The extension of the shock-expansion method to portions of wings made up of cones - or, if desired, convolutes - is the subject of the present paper.

As in the usual two-dimensional case, it is required in the present work that any shock wave associated with the leading edge of the wing be attached and that the flow just downstream of the wave be supersonic normal to the edge. If these conditions are met, the method then applies in those regions of the wing where (a) the component of velocity normal to the surface rulings is supersonic and (b) the flow is unaffected by the presence of tips or junctures. Such regions, though seemingly rather special, are of interest for two reasons. First, at the higher supersonic Mach numbers - say 3 and above - they may constitute a majority of the wing surface. Second, as will be seen below, the flow in these regions is of a simple type which is amenable to a relatively precise analysis. In particular, the flow quantities are (with a minor qualification in the case of the convolute) constant along the surface rulings.

The reasoning on which the foregoing statement is based is as follows: Consider that the surface of the wing is replaced by an inscribed polyhedron whose edges coincide with rulings of the actual surface.[1] In view of the single-curved nature of the surface, this can obviously be done. If the conditions of the preceding paragraph are satisfied, the flow at the leading edge of the wing will be characterized by an oblique shock wave or a yawed Prandtl-Meyer expansion. In either case the flow quantities will be constant on the face of the polyhedron adjoining the leading edge. At subsequent edges of the polyhedron where the component of velocity normal to the edge is supersonic, an expansion fan will originate. If one neglects the reflected effects that arise when these expansion fans interact with a leading-edge shock wave,[2] the fans themselves will be of the yawed Prandtl-Meyer type. To this approximation, therefore, the flow quantities will be constant on each face of the polyhedron. Now let the number of faces of the polyhedron increase indefinitely. In the limit the polyhedron will become the single-curved surface, and the faces of the polyhedron will become the surface rulings. It follows that, if reflected effects are neglected, the flow quantities must

[1]It will be assumed throughout that the surface is convex to the flow and free of sharp corners, though these restrictions are not essential.

[2]This approximation is also made in the two-dimensional case. The resulting errors are discussed by Eggers, Syvertson, and Kraus in reference 6. They conclude that in two-dimensional flow the errors are small except for conditions near shock detachment. There is no reason to expect that the situation will be substantially different in the present case.

be constant on each ruling. (In the case of the cone, where the shock wave and reflected effects are themselves conical, the qualification in this statement can be dropped, and the conclusion taken as exact. It can, in fact, be arrived at directly from the familiar argument concerning the lack of a characteristic length in the boundary-value problem in the conical case. For the convolute an argument like the foregoing is necessary, and the qualification must be retained. In the calculations that follow, as distinct from the argument itself, the reflected disturbances will always be ignored, and a quantitative approximation will remain in either case.)

The method of calculation is arrived at by simple extension of the foregoing ideas. To this end, we concentrate attention on an element of the polyhedron consisting of one corner and the adjoining downstream face and regard the angular deflection at the corner and the angular breadth of the face as infinitesimal. Since reflected effects are neglected, the expansion occurring at the corner can now be regarded as taking place through an infinitesimal plane wave (i.e., Mach wave) passing through the corner. The accompanying changes in flow are readily calculated from the fact that the vectorial change in velocity from one side of the wave to the other must be normal to the wave. Across the face of the element - that is, from one corner to the next - the only changes that need be considered are those associated with the change in relative orientation between the velocity (which is constant on the face) and the corners themselves. These changes, which affect the upstream conditions for the wave at the next corner, are found from simple considerations of geometry. Following this procedure, one obtains, in the limit of the curved surface, a pair of simultaneous, nonlinear ordinary differential equations for the components of Mach number normal and tangential to the surface rulings. These equations are to be integrated from the leading edge rearward. The Mach number components at the leading edge, which provide the initial conditions for the integration, are found by applying the concepts of simple-sweep theory to the equations for an oblique shock wave or Prandtl-Meyer expansion. The integration itself is readily accomplished by standard numerical means.

The first section of the paper is concerned mainly with the derivation of the differential equations and with the evaluation of certain derivatives required for their application to conical surfaces. The second section discusses the simplifications that occur when the usual small-disturbance approximations are introduced, both in the linear supersonic range and at hypersonic speeds. Of particular interest here is the result that at hypersonic speeds the method reduces to a simple strip theory in the streamwise direction. In this section of the paper a closed expression is also obtained for the pressure distribution on conical wings of biconvex section in the linear case. The paper concludes with some numerical results for a triangular wing made up of conical surfaces with apex at the tip. A realization that the pressures on a portion of this wing must be constant on rays through the tip was, in fact, the starting point of the analysis.

Although the present problem is a fairly obvious one, reference to it in existing literature is difficult to find. The only paper the authors have come upon, in fact, is that of Thomson and Sheppard (ref. 7), which became available after the present analysis was complete. In this reference, the surface of a conical wing is approximated by a polyhedron and the pressure distribution on this approximating surface calculated by application of simple-sweep theory and the Prandtl-Meyer relations at each successive corner. The present plan of incorporating a limiting process may be preferable with regard to accuracy and ease of computation.[3]

NOTATION

Primary Symbols

a	speed of sound
c	wing chord (measured at arbitrary spanwise station)
C_p	pressure coefficient (see eq. (30))
$f(\xi/c)$	function defining shape of wing section
$\vec{M}$	Mach number vector
M	magnitude of Mach number vector
p	static pressure
p_t	total pressure
r	radial distance along surface ruling
t	thickness of wing section
T	absolute temperature
v	magnitude of disturbance velocity, $V - V_\infty$
$\vec{V}$	velocity vector

[3]For the calculation of the entire nonlinear flow field around a general conical surface, reference should be made to the work of Maslen (ref. 8). The same problem has also been discussed by Ferri at the Conference on High Speed Aerodynamics, Polytechnic Institute of Brooklyn, January 20-22, 1955.

V magnitude of velocity vector

δV increment in V

x,y,z Cartesian coordinates

α angle of attack measured in streamwise direction

α_n angle of attack measured in plane normal to leading edge

γ ratio of specific heats (7/5 for air)

δ_n deflection angle measured in plane normal to leading edge

ζ,η local Cartesian coordinates in plane normal to surface ruling (see sketch (d))

λ leading-edge angle measured in streamwise direction

λ_n leading-edge angle measured in plane normal to leading edge

μ_n Mach angle corresponding to component of velocity normal to surface ruling

ν angle between velocity vector and surface ruling (see sketch (a))

ξ chordwise position aft of leading edge at arbitrary spanwise station

$\delta\sigma$ infinitesimal angle between two edges of face of polyhedron (see sketch (b))

$\delta\tau$ infinitesimal deflection angle at corner of polyhedron measured in plane normal to corner (see sketch (b))

$\frac{d\sigma}{d\omega}$ rate of rotation, at a given ruling, of the orthogonal projection of a moving surface ruling onto a fixed tangent plane through the given ruling

$\frac{d\tau}{d\omega}$ rate of rotation, at a given ruling, of a moving tangent plane, measured in a plane normal to the ruling

φ,ω angles used to specify position of rulings on conical surface (see sketch (c))

Subscripts

∞ conditions in free stream

*	conditions at critical speed
o	values at origin of ζ,η coordinate system (see sketch (d))
1	values at leading edge
2	values at trailing edge
n	component of velocity or Mach number normal to surface ruling (see sketch (a))
t	component of velocity or Mach number tangential to surface ruling (see sketch (a))
C	change across corner of polyhedron (see sketch (b))
F	change across face of polyhedron (see sketch (b))

Superscripts

$( )'$	first derivative of function with respect to argument
$( )''$	second derivative of function with respect to argument

SHOCK-EXPANSION METHOD

Differential Equations for Flow Over Single-Curved Surface

Since the flow along a solid boundary must be everywhere tangent to the boundary, the velocity vector $\vec{V}$ at any point on a single-curved surface will be completely defined if the magnitudes V_n and V_t of its components normal and tangential to the surface ruling at that point are known (sketch (a)). In the present case, where $\vec{V}$ is constant on each ruling, V_n and V_t are given by a pair of ordinary differential equations that can be derived as follows:

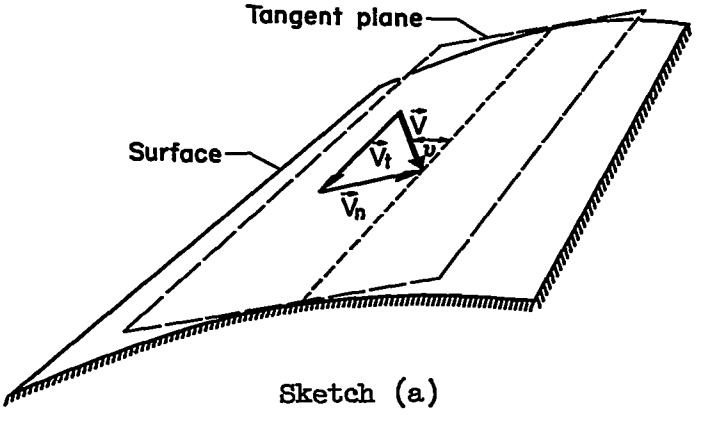

Sketch (a)

As explained in the introduction, we begin by regarding the single-curved surface as the limit of a polyhedron whose edges coincide with rulings of the actual surface. Let us then consider the flow over an

infinitesimal element of the polyhedron (sketch (b)) consisting of a corner C and the adjoining downstream face F. The infinitesimal deflection at the corner, measured in a plane normal to the corner, is denoted by $\delta\tau$. The infinitesimal angle between the two edges of the face F is represented by $\delta\sigma$. (The positive directions of $\delta\tau$ and $\delta\sigma$ are shown in the sketch.) The changes in V_n and V_t across the complete element C plus F will be considered as composed of the changes across the corner C followed by the changes across the face F.

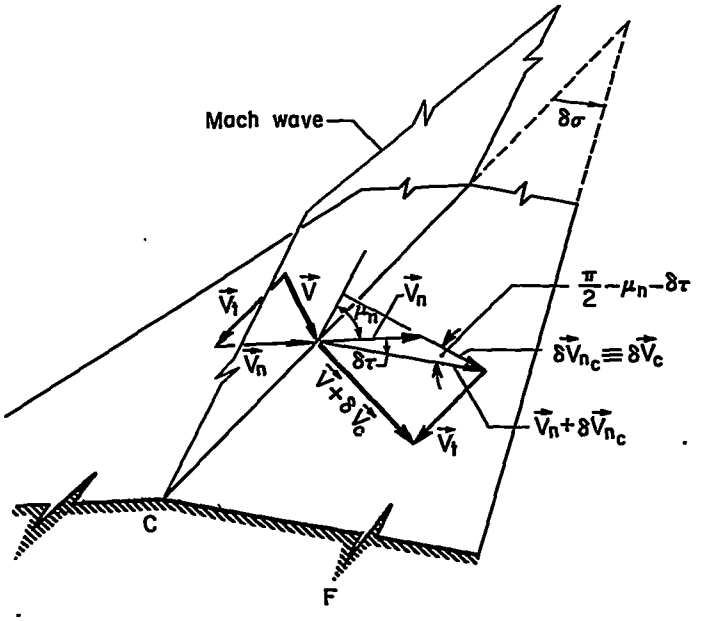

Sketch (b)

Under the conditions discussed in the introduction, the changes across the corner C will take place through a planar Mach wave originating at the corner. Let V, V_n, and V_t here denote the magnitudes of the velocity and its normal and tangential components upstream of the corner. According to the properties of infinitesimal plane waves, the angle between the Mach wave and the upstream face of the corner is then given by

$$\mu_n = \tan^{-1}\frac{1}{\sqrt{\frac{V_n^2}{a^2}-1}} \tag{1}$$

where a is the speed of sound corresponding to V. The situation downstream of the corner (see sketch (b)) is completely determined by (a) the property that the vectorial change in velocity $\delta\vec{V}_C$ across the corner must be normal to the wave and (b) the boundary condition that the resultant velocity $\vec{V}+\delta\vec{V}_C$ downstream of the corner must be parallel to the face F. From requirement (a) it follows at once that the change in V_t across the corner is zero, that is,

$$\delta V_{t_C} = 0 \tag{2}$$

The corresponding change in V_n can be found by considering the triangle formed by the vectors $\vec{V}_n$, $\delta\vec{V}_{n_C}(\equiv\delta\vec{V}_C)$, and $\vec{V}_n+\delta\vec{V}_{n_C}$. From this triangle, whose geometry is dictated by requirements (a) and (b), it follows that

$$\frac{V_n + \delta V_{n_C}}{V_n} = \frac{\sin\left(\frac{\pi}{2} + \mu_n\right)}{\sin\left(\frac{\pi}{2} - \mu_n - \delta\tau\right)}$$

With the aid of equation (1), this can be written, to the first order in infinitesimal quantities,

$$\delta V_{n_C} \cong \frac{V_n}{\sqrt{\frac{V_n^2}{a^2} - 1}}\,\delta\tau \tag{3}$$

This is, of course, identical to the corresponding equation for two-dimensional Prandtl-Meyer flow (cf. ref. 9) except for the appearance of V_n where V would ordinarily be.

The changes in V_n and V_t across the face F are found from the fact that the velocity vector is constant in magnitude and direction on the face. If ν is the angle between this vector and the surface ruling (see sketch (a)), we have in general

$$V_n = V \sin \nu$$

$$V_t = V \cos \nu$$

Differentiation of these expressions gives, for constant V,

$$\left.\begin{aligned} dV_n &= V \cos \nu \, d\nu = V_t d\nu \\ dV_t &= -V \sin \nu \, d\nu = -V_n d\nu \end{aligned}\right\} \tag{4}$$

Since the direction of the velocity vector does not vary on F, the change in ν from one edge to the other is due solely to the difference in orientation of the edges. Application of equations (4) to the calculation of the changes in V_n and V_t across F thus gives to the first order (and with due regard for the positive direction of $\delta\sigma$)

$$\delta V_{n_F} \cong -V_t \delta\sigma \tag{5}$$

$$\delta V_{t_F} \cong (V_n + \delta V_{n_C})\delta\sigma \cong V_n \delta\sigma \tag{6}$$

The changes in flow across the complete element C plus F can now be found by combining equations (2) and (6), and (3) and (5). In this manner we obtain, in the limit as the infinitesimal quantities tend to zero, the following ordinary differential equations for the calculation of the flow over a single-curved surface:

$$dV_n = \frac{V_n}{\sqrt{\frac{V_n^2}{a^2} - 1}} d\tau - V_t d\sigma \tag{7a}$$

$$dV_t = V_n d\sigma \tag{7b}$$

For computational work it is convenient to rewrite the above equations in dimensionless form in terms of the normal and tangential Mach numbers M_n and M_t, where $M_n \equiv V_n/a$ and $M_t \equiv V_t/a$.[4] To do this the defining expressions for M_n and M_t are first differentiated to obtain

$$dM_n = \frac{dV_n}{a} - M_n \frac{da}{a} \tag{8a}$$

$$dM_t = \frac{dV_t}{a} - M_t \frac{da}{a} \tag{8b}$$

The speed of sound a is known to be related to the Mach number by the adiabatic energy equation, which can be written (cf. ref. 10, eq. (32b))

$$\left(\frac{a}{a_*}\right)^2 = \frac{\gamma + 1}{2}\left[1 + \frac{\gamma - 1}{2}\left(M_n^2 + M_t^2\right)\right]^{-1}$$

where a_* is the constant critical speed. Differentiation of this relation gives

$$\frac{da}{a} = -\frac{\gamma - 1}{2} \frac{M_n dM_n + M_t dM_t}{1 + \frac{\gamma - 1}{2}\left(M_n^2 + M_t^2\right)}$$

[4]The analysis could be simplified at this point by making the speeds dimensionless through division by the constant critical speed a_* instead of by the variable speed of sound a. This leads, however, to slightly increased labor in the eventual numerical work.

The desired differential equations are now found by substituting this expression and equations (7) into equations (8) and solving for dM_n and dM_t. This gives finally

$$dM_n = \frac{M_n\left(1 + \frac{\gamma - 1}{2} M_n^2\right)}{\sqrt{M_n^2 - 1}} d\tau - M_t d\sigma \tag{9a}$$

$$dM_t = \frac{\gamma - 1}{2} \frac{M_n^2 M_t}{\sqrt{M_n^2 - 1}} d\tau + M_n d\sigma \tag{9b}$$

The differential equations (9) provide a means for calculating the Mach number (and hence the pressure) distribution on a single-curved surface under the conditions outlined in the introduction. To integrate the equations for a given surface, the differentials $d\tau$ and $d\sigma$ must be rewritten in the form $d\tau = (d\tau/dA)dA$ and $d\sigma = (d\sigma/dA)dA$, where A is any independent variable by which the position of the surface rulings can be conveniently defined. In the light of the limiting process, the derivatives $d\tau/dA$ and $d\sigma/dA$ can be given simple geometrical interpretations in terms of the rulings and tangent planes of the curved surface. The derivative $d\tau/dA$ at a given ruling can be identified as the rate of rotation of a moving tangent plane, evaluated at the ruling in question and measured in a plane normal to the ruling. The derivative $d\sigma/dA$ is the corresponding rate of rotation of the orthogonal projection of a moving surface ruling onto the (fixed) tangent plane through the given ruling. Expressions for these derivatives for a general conical surface are given (for a suitable choice of A) in the next section of the paper. The actual integration can be carried out by any one of a number of standard, step-by-step numerical procedures, depending on the accuracy required (see, e.g., refs. 11 and 12). Obviously, the integration breaks down when $M_n \leqq 1$.

It is important to note that the following sign conventions are implicit in the derivation of equations (9): (a) M_n is positive when $\vec{V}_n$ is in the direction of positive $d\sigma$ (see sketch (b)); (b) M_t is positive when $\vec{V}_t$ is directed away from the intersection of the surface rulings. These conventions must be carefully observed in carrying out the numerical integration.

Equations (9) are, of course, applicable to the swept cylinder as well as the cone and the convolute. In this case $d\sigma$ is identically zero, and M_n becomes independent of M_t (see eq. (9a)). This is as it should be according to the concepts of simple-sweep theory (ref. 13).

For such a problem, however, the methods of the present paper are superfluous, since a solution is readily found from tabular results for two-dimensional flow (see, e.g., ref. 14).

Application to Concial Surfaces

In the following section equations (9) will be specialized to a conical surface, since this is the case most commonly encountered in practice. For such a surface, the position of the rulings - and hence the shape of the cone - can be specified by an equation of the form

$$\varphi = \varphi(\omega) \tag{10}$$

where φ and ω are as indicated in sketch (c). Here x, y, and z are Cartesian coordinates fixed in the wing, with origin O at the apex of the cone.[5] The x,z plane is taken as the chord plane of the wing. The velocity of the undisturbed stream is assumed parallel to the x,y plane. With ω as the independent variable (replacing A of the preceding section), equations (9) can be written

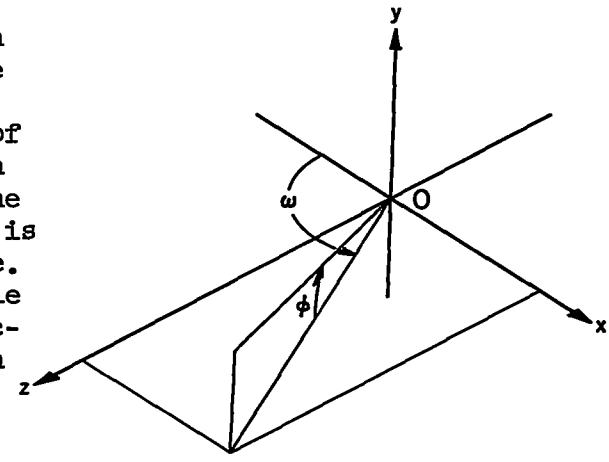

Sketch (c)

$$dM_n = \left[\frac{M_n\left(1 + \frac{\gamma - 1}{2} M_n^2\right)}{\sqrt{M_n^2 - 1}} \frac{d\tau}{d\omega} - M_t \frac{d\sigma}{d\omega}\right] d\omega \tag{11a}$$

$$dM_t = \left[\frac{\frac{\gamma - 1}{2} M_n^2 M_t}{\sqrt{M_n^2 - 1}} \frac{d\tau}{d\omega} + M_n \frac{d\sigma}{d\omega}\right] d\omega \tag{11b}$$

[5]This apex may be located at either the tip or forwardmost point of the wing. In the case of a wing with a truncated tip, the apex may be virtual rather than actual.

The task now is the purely geometrical one of expressing $d\tau/d\omega$ and $d\sigma/d\omega$ in terms of the known function $\varphi(\omega)$.

To do this let us consider a representative surface ruling at ω_o, φ_o. At a point o located a radial distance r_o along this ruling (see sketch (d)), we establish a rectangular coordinate system ζ,η in a

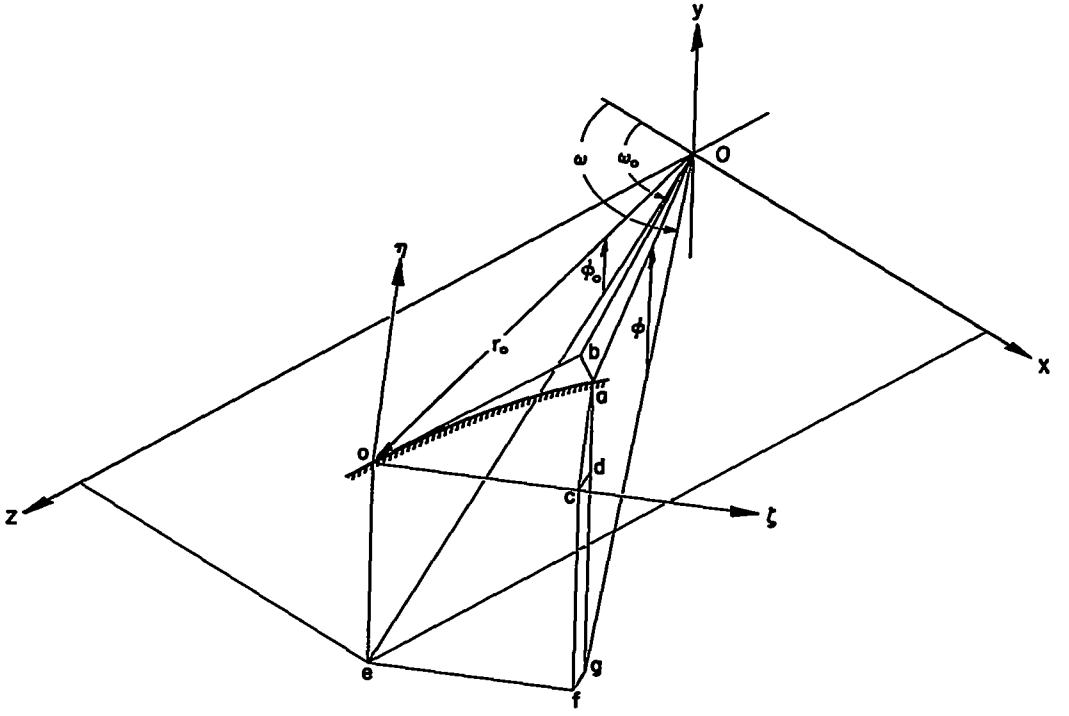

Sketch (d)

plane normal to the ruling. The ζ direction is taken parallel to the x,z plane with ζ positive in the direction of increasing ω; η is positive in the direction of increasing φ. The trace of the conical surface in the ζ,η plane is then given by an equation of the form

$$\eta = \eta(\zeta)$$

Expressions for τ and σ are now needed for differentiation. Recalling the geometrical interpretation of the derivative of τ following equations (9), we can write (with due regard for the positive direction of $\delta\tau$ as shown in sketch (b))

$$\tau = \tan^{-1}\left(\frac{d\eta}{d\zeta}\right)_o - \tan^{-1}\left(\frac{d\eta}{d\zeta}\right) \tag{12}$$

where the subscript o denotes evaluation at the point o. To write an expression for σ, we consider an arbitrary point a on the trace of the conical surface. Let the point b be the orthogonal projection of a onto the trace (in the ζ,η plane) of the tangent plane to the conical surface at the ruling o0. In the light of the previous interpretation of the derivative of σ, we can then write

$$\sigma = \tan^{-1} \frac{\overline{ob}}{r_o}$$

An expression for $\overline{ob}$ can be obtained by considering the planar figure obac, where c is the orthogonal projection of a onto the ζ axis. Since $\overline{oc} = \zeta$ and $\overline{ac} = \eta$, we have

$$\overline{ob} = \zeta \cos\left[\tan^{-1}\left(\frac{d\eta}{d\zeta}\right)_o\right] + \eta \sin\left[\tan^{-1}\left(\frac{d\eta}{d\zeta}\right)_o\right] = \frac{\zeta + \eta\left(\frac{d\eta}{d\zeta}\right)_o}{\sqrt{1 + \left(\frac{d\eta}{d\zeta}\right)_o^2}}$$

The expression for σ can thus be written

$$\sigma = \tan^{-1} \frac{\zeta + \eta\left(\frac{d\eta}{d\zeta}\right)_o}{r_o\sqrt{1 + \left(\frac{d\eta}{d\zeta}\right)_o^2}} \tag{13}$$

Expressions (12) and (13) must now be differentiated with respect to ω, and the derivatives evaluated at the point o. Since η and ζ will be expressed subsequently as functions of ω, the resulting expressions will be put in terms of derivatives with respect to this quantity. We thus obtain

$$\left(\frac{d\tau}{d\omega}\right)_o = -\frac{\left(\frac{d\zeta}{d\omega}\right)_o\left(\frac{d^2\eta}{d\omega^2}\right)_o - \left(\frac{d\eta}{d\omega}\right)_o\left(\frac{d^2\zeta}{d\omega^2}\right)_o}{\left(\frac{d\zeta}{d\omega}\right)_o^2 + \left(\frac{d\eta}{d\omega}\right)_o^2} \tag{14a}$$

$$\left(\frac{d\sigma}{d\omega}\right)_o = \frac{1}{r_o}\sqrt{\left(\frac{d\zeta}{d\omega}\right)_o^2 + \left(\frac{d\eta}{d\omega}\right)_o^2} \tag{14b}$$

Expressions for ζ and η as functions of ω can be found by returning to sketch (d). The points e, f, and g are first established as the orthogonal projections of o, c, and a onto the x,z plane. The point d is then established on the line ag by drawing cd parallel to fg. From the geometry of the resulting figure, it is apparent that $\overline{ef} = \overline{oc} = \zeta$ and $\overline{fg} = \overline{cd} = \overline{ac} \sin \varphi_o = \eta \sin \varphi_o$. We can therefore write, from consideration of the quadrilateral efgO,

$$\tan(\omega - \omega_o) = \frac{\overline{ef}}{\overline{eO} - \overline{fg}} = \frac{\zeta}{r_o \cos \varphi_o - \eta \sin \varphi_o} \tag{15}$$

and

$$\sin(\omega - \omega_o) = \frac{\overline{ef}}{\overline{gO}} = \frac{\zeta}{\overline{gO}} \tag{16}$$

An expression for $\overline{gO}$ is found by observation of the triangle gaO. Since $\overline{ad} = \overline{ac} \cos \varphi_o = \eta \cos \varphi_o$ and $\overline{dg} = \overline{cf} = \overline{oe} = r_o \sin \varphi_o$, it follows that

$$\tan \varphi = \frac{\overline{dg} + \overline{ad}}{\overline{gO}} = \frac{r_o \sin \varphi_o + \eta \cos \varphi_o}{\overline{gO}} \tag{17}$$

and hence by combination with equation (16) that

$$\frac{\sin(\omega - \omega_o)}{\tan \varphi} = \frac{\zeta}{r_o \sin \varphi_o + \eta \cos \varphi_o} \tag{18}$$

Equations (15) and (18) constitute a pair of simultaneous equations for ζ and η. Solution of these equations gives

$$\zeta = r_o \frac{\sin(\omega - \omega_o)}{\cos \varphi_o \cos(\omega - \omega_o) + \sin \varphi_o \tan \varphi} \tag{19a}$$

$$\eta = r_o \frac{\tan \varphi - \tan \varphi_o \cos(\omega - \omega_o)}{\cos(\omega - \omega_o) + \tan \varphi_o \tan \varphi} \tag{19b}$$

Since the relation (10) will be known in any given case, these equations give ζ and η as functions of ω.

Equations (19) must now be differentiated to find the quantities required in equations (14). This operation gives finally

$$\left(\frac{d\zeta}{d\omega}\right)_o = r_o \cos \varphi_o$$

$$\left(\frac{d\eta}{d\omega}\right)_o = r_o \varphi_o'$$

$$\left(\frac{d^2\zeta}{d\omega^2}\right)_o = -2r_o \varphi_o' \sin \varphi_o$$

$$\left(\frac{d^2\eta}{d\omega^2}\right)_o = r_o(\sin \varphi_o \cos \varphi_o + \varphi_o'')$$

where the primes denote differentiation of φ with respect to its argument. Substitution of these expressions into equations (14) gives, after the subscripts are dropped, the following relations for the required geometrical derivatives:

$$\frac{d\tau}{d\omega} = - \frac{\sin \varphi \cos^2 \varphi + \varphi'' \cos \varphi + 2\varphi'^2 \sin \varphi}{\cos^2 \varphi + \varphi'^2} \tag{20a}$$

$$\frac{d\sigma}{d\omega} = \sqrt{\cos^2 \varphi + \varphi'^2} \tag{20b}$$

With the aid of equations (20), the differential equations (11) can be integrated numerically for any conical wing for which φ is given as a function of ω.[6]

On most conical wings encountered in practice, the apex of the cone will be located at the wing tip. In this case the contour of the surface is usually defined by specifying the shape of the streamwise airfoil section - that is, by an equation of the form

$$\frac{y}{c} = \frac{t}{c} f\left(\frac{\xi}{c}\right) \tag{21}$$

where c is the chord of the wing at some arbitrary spanwise station z, ξ is the chordwise distance aft from the leading edge at that station, t/c is the thickness ratio of the airfoil section, and f is some given function of ξ/c. In an application of this type, it is advantageous to replace $d\omega$ in equations (11) by $[d\omega/d(\xi/c)]d(\xi/c)$ and integrate directly with respect to ξ/c. The necessary expression for $d\omega/d(\xi/c)$ can be found by reference to sketch (e). If ω_1 and ω_2 are the values of ω corresponding to the leading and trailing edges of the wing, it follows from the sketch that

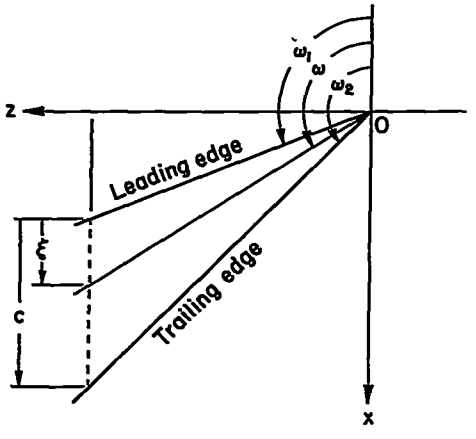

Sketch (e)

$$\xi = z\left(\frac{1}{\tan \omega_1} - \frac{1}{\tan \omega}\right) \tag{22a}$$

$$c = z\left(\frac{1}{\tan \omega_1} - \frac{1}{\tan \omega_2}\right) \tag{22b}$$

Elimination of z between these equations and solution for $\tan \omega$ gives

$$\tan \omega = \frac{\tan \omega_1}{1 - \frac{\xi}{c}\left(1 - \frac{\tan \omega_1}{\tan \omega_2}\right)} \tag{23}$$

[6]Dr. Stephen H. Maslen of the NACA Lewis Laboratory has pointed out to the authors that equations (11) and (20) can also be derived from the general differential equations for conical flow as given in reference 8.

from which it follows that

$$\frac{d\omega}{d(\xi/c)} = \frac{\sin^2\omega}{\tan\omega_1}\left(1 - \frac{\tan\omega_1}{\tan\omega_2}\right) \tag{24}$$

To find φ as a function of ξ/c, reference is made to sketch (c). This gives

$$\tan\varphi = \frac{y}{z/\sin\omega}$$

which becomes, with the aid of equations (21) and (22b),

$$\tan\varphi = \frac{t}{c}\frac{\sin\omega}{\tan\omega_1}\left(1 - \frac{\tan\omega_1}{\tan\omega_2}\right)f\left(\frac{\xi}{c}\right) \tag{25}$$

Equations (20), (23), (24), and (25) provide the relations necessary to integrate equations (11) as functions of ξ/c.

Initial Conditions

The initial conditions for the integration of equations (9) or (11) are the values of the Mach number components at the leading edge. These values, denoted by M_{n_1} and M_{t_1}, are found by applying the concepts of simple-sweep theory (ref. 13) to the locally cylindrical flow at the edge.

The situation is as shown in sketch (f).[7] The given quantities are the magnitude M_∞ of the free-stream Mach number, the angle of attack α, the angular location ω_1 of the leading edge, and the leading-edge angle λ measured parallel to the x,y plane. To

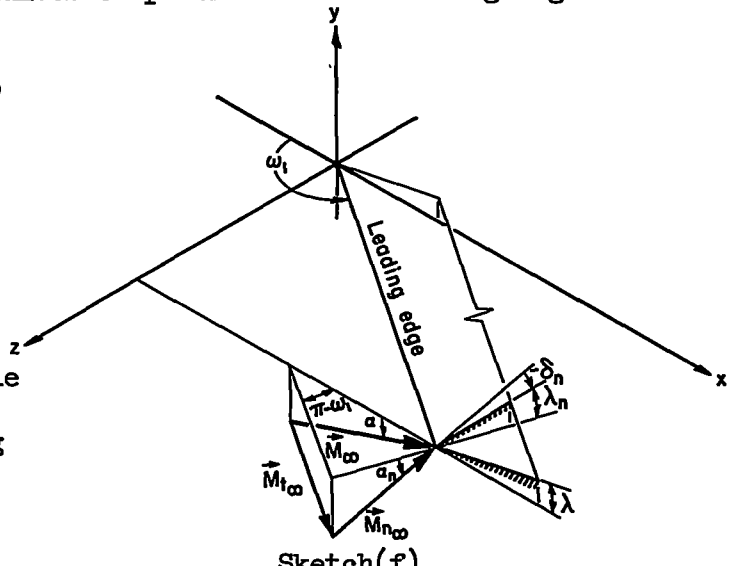

Sketch(f)

[7]To understand this sketch it should be recalled that the vector $\vec{M}_\infty$ is parallel to the x,y plane.

apply simple-sweep theory, one must know the magnitudes M_{n_∞} and M_{t_∞} of the components of free-stream Mach number normal and tangential to the leading edge together with the deflection angle δ_n measured in a plane normal to the edge. As can be seen from the figure, the Mach number components are given by

$$M_{t_\infty} = M_\infty \cos \alpha \cos(\pi - \omega_1)$$

$$= -M_\infty \cos \alpha \cos \omega_1 \tag{26a}$$

and

$$M_{n_\infty} = \sqrt{M_\infty^2 - M_{t_\infty}^2}$$

$$= M_\infty \sqrt{1 - \cos^2\alpha \cos^2\omega_1} \tag{26b}$$

The deflection angle (taken as positive when the deflection causes a compression) is given by

$$\delta_n = \lambda_n - \alpha_n \tag{27}$$

where λ_n and α_n are the leading-edge angle and the angle of attack, both measured in a plane normal to the edge. These angles are related to the given angles by the following equations (readily derived on the basis of the sketch):

$$\alpha_n = \tan^{-1}\left(\frac{\tan \alpha}{\sin \omega_1}\right) \tag{28a}$$

$$\lambda_n = \tan^{-1}\left(\frac{\tan \lambda}{\sin \omega_1}\right) \tag{28b}$$

With M_{n_∞} and δ_n known, the value of M_{n_1} is easily found from the well-known results for an oblique shock wave ($\delta_n > 0$) or Prandtl-Meyer expansion ($\delta_n < 0$). (See, e.g., refs. 5, 10, or 15.) As required by simple-sweep theory, the calculations are carried out in the same manner as for two-dimensional flow (see ref. 15), except that "normal" quantities are used in place of the usual resultant values. The value of M_{t_1} is found from the fact, given by simple-sweep theory, that V_t at the leading edge is the same as in the free stream, that is,

$$V_{t_1} = V_{t_\infty}$$

Division of this equation by the speed of sound a_1 gives

$$\frac{V_{t_1}}{a_1} = \frac{V_{t_\infty}}{a_1} = \frac{V_{t_\infty}}{a_\infty}\frac{a_\infty}{a_1}$$

or finally

$$M_{t_1} = \frac{M_{t_\infty}}{(a_1/a_\infty)} = \frac{M_{t_\infty}}{\sqrt{T_1/T_\infty}} \tag{29}$$

The value of M_{t_∞} is given by equation (26a). The value of a_1/a_∞ or T_1/T_∞ is found from two-dimensional theory as before (see ref. 15).

As a general remark, it may be noted that the angle of attack enters the entire scheme of calculation only through its influence on the initial conditions. The differential equations (9) and (11), and the derivatives that appear therein, are all independent of α.

Pressure Coefficient

The value of the local pressure coefficient

$$C_p \equiv \frac{2}{\gamma M_\infty^2}\left(\frac{p}{p_\infty} - 1\right) \tag{30}$$

is easily found once the distributions of M_n and M_t are known. To find p/p_∞ - and hence C_p - we distinguish two cases as follows:

$\underline{\delta_n < 0}$.- In this case there is an expansion at the leading edge and the flow is isentropic. The total pressure is therefore everywhere the same, and we can write

$$\frac{p}{p_\infty} = \frac{(p/p_t)}{(p/p_t)_\infty} \tag{31}$$

The values of $(p/p_t)_\infty$ and (p/p_t) are found from the usual compressible-flow tables (e.g., ref. 10) as functions of M_∞ and M, where $M = \sqrt{M_n^2 + M_t^2}$.

$\delta_n > 0$.- In this case, because of the increase in entropy through the leading-edge shock, it cannot be said that $p_t = p_{t_\infty}$. We can, however, write that $p_t = p_{t_1}$ and hence that

$$\frac{p}{p_\infty} = \frac{(p_1/p_\infty)}{(p/p_t)_1}\left(\frac{p}{p_t}\right) \tag{32}$$

The values of $(p/p_t)_1$ and (p/p_t) can be obtained from the compressible-flow tables as functions of the corresponding Mach number. The value of (p_1/p_∞) is found, as before, from an oblique-shock calculation based on the flow normal to the leading edge.

SMALL-DISTURBANCE APPROXIMATION

It is of interest to examine the form the analysis takes when the small-disturbance approximations are introduced. To this end we define a disturbance speed v according to the relation

$$V = V_\infty + v \tag{33}$$

and assume that terms of higher than the first order in v/V_∞ can be neglected. Consistent with this approach, we also assume that the wing surface $y = y(x,z)$ lies sufficiently close to the x,z plane that only first-order terms in y and its derivatives need be retained.

General Small-Disturbance Equation

To incorporate the foregoing assumptions into the analysis, we return to the differential equations (7) and rewrite them in terms of the resultant velocity V. This is done by means of the relation

$$V^2 = V_n^2 + V_t^2$$

which becomes after differentiation

$$V\,dV = V_n\,dV_n + V_t\,dV_t$$

By substitution of the expressions for dV_n and dV_t from equations (7), the following differential equation for V is obtained:

$$\frac{dV}{V} = \frac{V_n^2}{V^2\sqrt{\frac{V_n^2}{a^2} - 1}}\,d\tau \tag{34}$$

The speed of sound a is related to V by the adiabatic energy equation, which can be written

$$a^2 = a_\infty^2\left\{1 - \frac{\gamma - 1}{2}M_\infty^2\left[\left(\frac{V}{V_\infty}\right)^2 - 1\right]\right\} \tag{35}$$

Now let us simplify equation (34) in the light of the previous assumptions. To begin, it can be shown that to a first order in small quantities

$$d\tau = -\frac{1}{\sin\omega}\,d\left(\frac{\partial y}{\partial x}\right)$$

Here ω again denotes the azimuthal angle of the surface ruling (cf. sketch (c)), though the considerations are not now restricted to a cone. To the same accuracy, the normal velocity V_n can be written

$$V_n = V_\infty\sin\omega + (\text{terms of first order})$$

where the form of the first-order terms is immaterial for present purposes. To the first order in v/V_∞, equation (35) also simplifies to

$$a^2 = a_\infty^2\left[1 - (\gamma - 1)M_\infty^2\,\frac{v}{V_\infty}\right]$$

If these three expressions are substituted into equation (34) and the assumption is made that $M_\infty\sin\omega \gg 1$ (i.e., the component of free-stream Mach number normal to the rulings is not near 1), one then obtains to the first order

$$d\left(\frac{v}{V_\infty}\right) = -\frac{\sin\omega}{\sqrt{\dfrac{M_\infty^2\sin^2\omega}{1-(\gamma-1)M_\infty^2\dfrac{v}{V_\infty}}-1}}\,d\left(\frac{\partial y}{\partial x}\right) \tag{36}$$

This equation is general in the sense that it contains both the linearized-supersonic and hypersonic approximations. These two approximations will now be discussed separately.

Linear Approximation

If M_∞ is not too large, we can write that $(\gamma - 1)M_\infty^2 \frac{v}{V_\infty} \ll 1$, and equation (36) simplifies immediately to

$$d\left(\frac{v}{V_\infty}\right) = -\frac{\sin\omega}{\sqrt{M_\infty^2\sin^2\omega - 1}}\,d\left(\frac{\partial y}{\partial x}\right) \tag{37}$$

This result is linear in that the distributions of v/V_∞ over two single-curved surfaces of identical plan form - say $y_1(x,z)$ and $y_2(x,z)$ - will upon being added equal the distribution of v/V_∞ over a third surface $y_3(x,z)$ where $y_3 = y_1 + y_2$. It is easily verified that equation (37) conforms to the similarity rules of linearized supersonic wing theory. Any velocity distribution calculated by means of this equation must, in fact, be identical to that which would be obtained by solution of the partial differential equation of linear theory under the same boundary conditions. This follows from the fact that the only phenomena specifically neglected in the present development - that is, the disturbances reflected from a leading-edge shock wave - disappear in the conventional linear development as well. Equation (37) will be integrated for a specific type of wing (i.e., for a specific relation between $\partial y/\partial x$ and ω) following a discussion of the hypersonic approximation.

Hypersonic Approximation

When M_∞ is very large, it can no longer be said that $(\gamma - 1)M_\infty^2 \frac{v}{V_\infty} \ll 1$. In this case, however, the first term under the radical in equation (36) will predominate, and the equation can be reduced to

$$\frac{M_\infty d\left(\frac{v}{V_\infty}\right)}{\sqrt{1 - (\gamma - 1)M_\infty^2 \frac{v}{V_\infty}}} = - d\left(\frac{\partial y}{\partial x}\right) \tag{38}$$

The dependence on ω thus disappears from the differential equation. Equation (38) is, in fact, the same equation one obtains if the hypersonic small-disturbance approximation is applied to the differential equation for two-dimensional Prandtl-Meyer flow.[8] The same situation can be shown to exist with regard to the calculation of the initial conditions and the pressure coefficient - that is, the equations are independent of ω and are the same as those obtained from the two-dimensional small-disturbance theory of hypersonic flow. It thus appears that, for thin wings at high Mach numbers, the pressure distribution can be found by disregarding the taper and treating the wing section from a simple two-dimensional point of view. This result is in agreement with the ideas expressed by Eggers in reference 16. It is a consequence, of course, of the fact that when the surface Mach number is everywhere large, as will be the case on a thin wing at a large free-stream Mach number, the region of dependence of a given point on the wing surface is of negligible extent in the spanwise direction.

Since ω does not appear in equation (38), the integration can be carried out at once. This will not be done here, since the results can be shown to agree with the equations for thin two-dimensional airfoils at hypersonic speeds as worked out completely by Linnell (ref. 17). These equations are arrived at by Linnell by making suitable approximations in the usual two-dimensional shock-expansion relations. According to present considerations, these approximate two-dimensional results may be applied directly to the streamwise sections of sufficiently thin tapered wings. For engineering applications to thicker wings, one might go a step farther and apply the complete shock-expansion method in the same manner. This latter possibility will be examined in the subsequent example.

Application of Linear Approximation to Conical Biconvex Wing

The linear approximation (37) will now be applied to a conical wing with apex of the cone located at the wing tip. For such a wing the surface is given by equation (21) as

[8]It can be shown that equation (38) conforms to the hypersonic similarity rules.

$$\frac{y}{c} = \frac{t}{c} f\left(\frac{\xi}{c}\right)$$

This can be differentiated to obtain

$$\frac{\partial y}{\partial x} = \frac{\partial(y/c)}{\partial(x/c)} = \frac{\partial(y/c)}{\partial(\xi/c)} = \frac{t}{c} f'\left(\frac{\xi}{c}\right)$$

and

$$d\left(\frac{\partial y}{\partial x}\right) = \frac{t}{c} f''\left(\frac{\xi}{c}\right) d\left(\frac{\xi}{c}\right) = \frac{t}{c} f''\left(\frac{\xi}{c}\right) \frac{d\omega}{d\omega/d(\xi/c)}$$

where the primes denote differentiation of f with respect to its argument. Substitution of the last relation into equation (37) and insertion of $d\omega/d(\xi/c)$ from equation (24) then gives for the governing differential equation

$$d\left(\frac{v}{V_\infty}\right) = -\left(\frac{t}{c}\right) \frac{\tan \omega_1}{1 - \frac{\tan \omega_1}{\tan \omega_2}} \frac{f''(\xi/c)}{\sin \omega \sqrt{M_\infty^2 \sin^2 \omega - 1}} d\omega$$

Since in linearized wing theory the pressure coefficient is given by $C_p = -2v/V_\infty$, one can also write

$$dC_p = 2\left(\frac{t}{c}\right) \frac{\tan \omega_1}{1 - \frac{\tan \omega_1}{\tan \omega_2}} \frac{f''(\xi/c)}{\sin \omega \sqrt{M_\infty^2 \sin^2 \omega - 1}} d\omega$$

If C_{p_1} is the pressure coefficient on the upper surface at the leading edge, it follows that the value of C_p at any other point on the same surface is given by

$$C_p = C_{p_1} + 2\left(\frac{t}{c}\right) \frac{\tan \omega_1}{1 - \frac{\tan \omega_1}{\tan \omega_2}} \int_{\omega_1}^{\omega} \frac{f''(\xi/c)}{\sin \omega \sqrt{M_\infty^2 \sin^2 \omega - 1}} d\omega \qquad (39)$$

The value of C_{p_1} can be found by applying simple-sweep concepts to the known results for linearized two-dimensional flow. This gives

$$C_{p_1} = \frac{2 \sin \omega_1}{\sqrt{M_\infty^2 \sin^2 \omega_1 - 1}} \left[\frac{t}{c} f'(0) - \alpha \right] \tag{40}$$

On a wing of biconvex section, $f''(\xi/c)$ is constant. (This is exactly true if the section is made up of parabolic arcs and true to the accuracy of small-disturbance theory if it is made up of circular arcs.) Equation (39) can then be written

$$C_p = C_{p_1} + 2\left(\frac{t}{c}\right) \frac{f'' \tan \omega_1}{1 - \frac{\tan \omega_1}{\tan \omega_2}} \int_{\omega_1}^{\omega} \frac{d\omega}{\sin \omega \sqrt{M_\infty^2 \sin^2 \omega - 1}}$$

The integral in this equation can be put into a standard form by means of the substitution $\rho = \sin^2 \omega$. In this manner one obtains finally the following equation for the pressure coefficient on a conically tapered wing of biconvex section:

$$C_p = C_{p_1} + \frac{(t/c) f'' \tan \omega_1}{1 - \frac{\tan \omega_1}{\tan \omega_2}} \left[\sin^{-1} \frac{(M_\infty^2 + 1)\sin^2 \omega - 2}{(M_\infty^2 - 1)\sin^2 \omega} - \right.$$

$$\left. \sin^{-1} \frac{(M_\infty^2 + 1)\sin^2 \omega_1 - 2}{(M_\infty^2 - 1)\sin^2 \omega_1} \right] \tag{41}$$

The value of C_{p_1} is given by equation (40); ω is related to the more common variable ξ/c by equation (23). Equation (41) could be obtained, presumably, by the conventional methods of linearized conical-flow theory, though the authors are not aware that this has been done.

NUMERICAL EXAMPLE

Calculations have been carried out on the basis of the foregoing methods for a sweptback triangular wing of aspect ratio 4 (sketch (g)). The surface of the wing is tapered linearly from the root to the tip - that is, each half of the wing is a cone with apex at the wing tip. With the origin of coordinates at the right-hand tip, it follows that $\omega_1 = 45^\circ$ and $\omega_2 = 90^\circ$. The wing section, which is symmetrical about the chord line, is 5 percent thick with maximum thickness at midchord. It is composed of a circular arc from the leading edge to the midchord and a parabolic arc from the midchord to the trailing edge. The trailing edge is blunt with a thickness one-half the maximum thickness. The function $f(\xi/c)$ is therefore (cf. eq. (21))

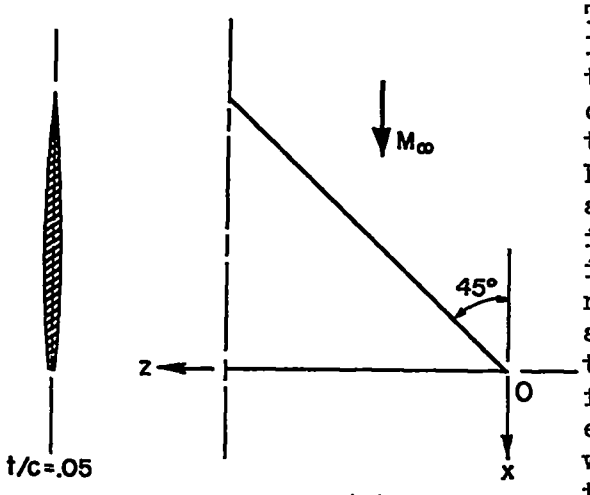

Sketch (g)

$$f\left(\frac{\xi}{c}\right) = \frac{1}{4(t/c)^2}\left(-\left[1-\left(\frac{t}{c}\right)^2\right] + \left\{\left[1-\left(\frac{t}{c}\right)^2\right]^2 - 16\left(\frac{t}{c}\right)^2\left(\frac{\xi}{c}\right)\left[\left(\frac{\xi}{c}\right)-1\right]\right\}^{\frac{1}{2}}\right)$$

for

$$0 \le \xi/c \le \frac{1}{2}$$

and

$$f\left(\frac{\xi}{c}\right) = \frac{1}{4} + \frac{\xi}{c} - \left(\frac{\xi}{c}\right)^2$$

for $1/2 \le \xi/c \le 1$. For this profile $f''(\xi/c)$ is seen to have a discontinuity at midchord.

The calculated values of C_p on the upper surface of the wing are shown in figure 1. Results are given for angles of attack of 0°, $\pm 3^\circ$, and $\pm 6^\circ$ at free-stream Mach numbers of 3.36 and 2.46. In each case, curves are shown as computed by the shock-expansion method of this report (eqs. (11)), by the corresponding linear approximation (eq. (41)), and by the ordinary (i.e., two-dimensional) shock-expansion method for the streamwise section. The numerical integration of equations (11) was carried out

in the present case by means of the simple "trapezoidal formula" (see, e.g., ref. 11, pp. 24-25 or ref. 12, pp. 236-238). Values given by this method with ten equal increments of ξ/c were amply accurate compared with results obtained by more refined methods of integration. The curves from the two-dimensional shock-expansion method are included in the figure for the reasons mentioned in the discussion of the hypersonic approximation. Sketches indicating the approximate regions of applicability of the results are shown for each Mach number. These regions, as approximated on the basis of the free-stream Mach angle, constitute 69 and 56 percent of the plan-form area at the respective Mach numbers of 3.36 and 2.46. More accurate determination of the regions as functions of M_∞ and α could, of course, be made on the basis of the results obtained in the pressure calculations themselves (cf. ref. 7). The value of α at which M_n becomes sonic just behind the leading-edge wave is -15.2° at $M_\infty = 3.36$ and -6.9° at $M_\infty = 2.46$.

The relationship observed in the present case between the shock-expansion results (solid curve) and the corresponding linear approximation (dashed curve) is much the same as that known for two-dimensional flow (cf. ref. 4, fig. E,3i). As in the latter case, the shock-expansion values of C_p are, with minor exceptions, more positive than the linear values by an amount which increases as the absolute value of C_p increases. As a consequence, the normal force on the wing at a given $|\alpha|$ (as indicated by the vertical distance between the C_p curves at equal $\pm\alpha$) is concentrated more toward the leading edge in the shock-expansion results. This effect would, of course, be less pronounced for wings of smaller thickness ratio.

Judged on the basis of the present shock-expansion findings, the curves obtained by the two-dimensional method are a good approximation at the positive angles of attack shown in figure 1. As the angle becomes negative, however, the approximation becomes progressively less accurate. This is due primarily to the error involved in the calculation of the discontinuous flow changes at the swept leading edge, an error which becomes larger as the absolute value of the deflection at the leading edge increases. On the present wing, this deflection is zero on the upper surface at $\alpha \cong 6^\circ$. The two-dimensional approximation would be expected to deteriorate again at positive angles greater than this value. This behavior is, of course, dependent on the amount of sweep at the leading edge. On a reversed triangular wing, for example, where the leading edge is unswept, the two-dimensional method would give accurate initial conditions at all angles, and the over-all situation would undoubtedly be different.

The logical argument for the use of the two-dimensional method in the present case rests, as has been seen, on the assumption that the free-stream Mach number is very large. The method would therefore be expected to diminish in accuracy as the Mach number is reduced. The results of figure 1 show this effect. It may be noted, however, that even at a moderate Mach number such as 3.36, the two-dimensional method provides remarkably good accuracy within the angle range studied here. This agrees with previous results (e.g., ref. 18) which show that other deductions based

on the hypersonic small-disturbance assumptions (as, e.g., the similarity rules) can be applied with good accuracy at fairly low supersonic Mach numbers.

Ames Aeronautical Laboratory
National Advisory Committee for Aeronautics
Moffett Field, Calif., April 8, 1955

REFERENCES

1. Warner, Frank Melville: Applied Descriptive Geometry. McGraw-Hill Book Co., Inc., 1934, pp. 88-89, 111-112.

2. Graustein, William C.: Differential Geometry. Macmillan Co., 1947, pp. 67-69.

3. Epstein, Paul S.: On the Air Resistance of Projectiles. Proc. Nat. Acad. Sci., vol. 17, 1931, pp. 532-547.

4. Lighthill, M. J.: Higher Approximations. Sec. E of General Theory of High Speed Aerodynamics, William R. Sears, ed., Princeton Univ. Press (Princeton), 1954, pp. 392-396.

5. Ivey, H. Reese, Stickle, George W., and Schuettler, Alberta: Charts for Determining the Characteristics of Sharp-Nose Airfoils in Two-Dimensional Flow at Supersonic Speeds. NACA TN 1143, 1947.

6. Eggers, A. J., Jr., Syvertson, Clarence A., and Kraus, Samuel: A Study of Inviscid Flow About Airfoils at High Supersonic Speeds. NACA Rep. 1123, 1953. (Supersedes NACA TN's 2646 and 2729.)

7. Thomson, K. D., and Sheppard, L. M.: The Application of Shock Expansion Theory to the Flow Outside Regions Influenced by the Apex or Tip on Wings With Supersonic Edges. Tech. Note HSA TN 11, High Speed Aerodynamics Lab., Adelaide, Australia, Mar. 1954.

8. Maslen, Stephen H.: Supersonic Conical Flow. NACA TN 2651, 1952.

9. Sauer, Robert: Introduction to Theoretical Gas Dynamics. Trans. by Freeman K. Hill and Ralph A. Alpher, J. W. Edwards (Ann Arbor), 1947, p. 87.

10. Staff of Ames Laboratory: Equations, Tables, and Charts for Compressible Flow. NACA Rep. 1135, 1953.

11. Milne, William Edmund: Numerical Solution of Differential Equations. John Wiley and Sons, Inc., 1953, pp. 19-98.

12. Scarborough, James Blaine: Numerical Mathematical Analysis. Johns Hopkins Press, 1950, pp. 235-306.

13. Busemann, A.: Aerodynamic Lift at Supersonic Speeds. 2844, Ae. Techl. 1201, British Aero. Res. Com., Feb. 3, 1947. (From Luftfahrtforschung, vol. 12, no. 6, Oct. 3, 1935, pp. 210-220.)

14. Ivey, H. Reese, and Bowen, Edward N., Jr.: Theoretical Supersonic Lift and Drag Characteristics of Symmetrical Wedge-Shape-Airfoil Sections as Affected by Sweepback Outside the Mach Cone. NACA TN 1226, 1947

15. Bonney, E. Arthur: Engineering Supersonic Aerodynamics. McGraw-Hill Book Co., Inc., 1950, pp. 79-103.

16. Eggers, A. J., Jr.: On the Calculation of Flow About Objects Traveling at High Supersonic Speeds. NACA TN 2811, 1952.

17. Linnell, Richard D.: Two-Dimensional Airfoils in Hypersonic Flows. Jour. Aero. Sci., vol. 16, no. 1, Jan. 1949, pp. 22-30.

18. Ehret, Dorris M., Rossow, Vernon J., and Stevens, Victor I., Jr.: An Analysis of the Applicability of the Hypersonic Similarity Law to the Study of Flow About Bodies of Revolution at Zero Angle of Attack. NACA TN 2250, 1950.

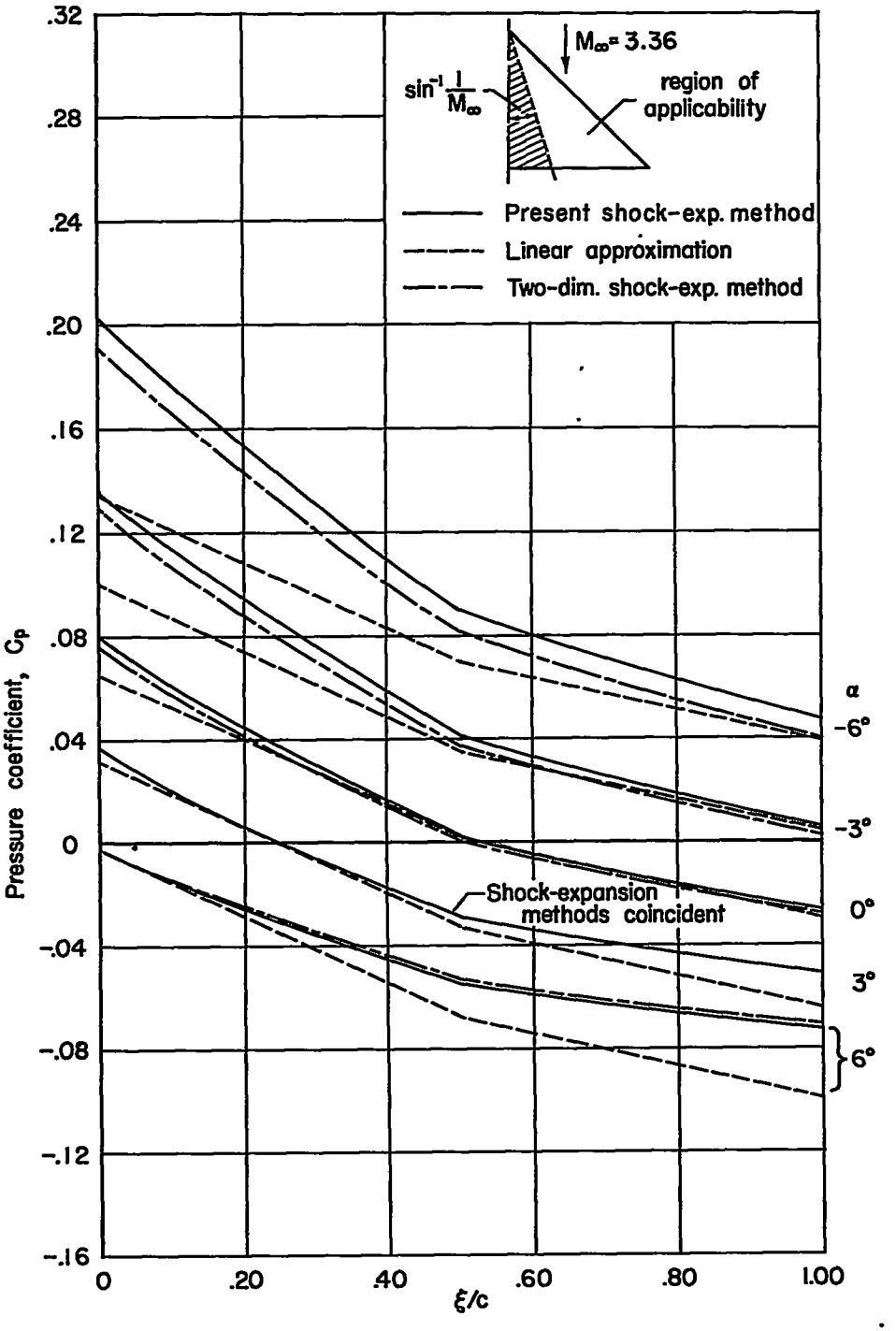

(a) $M_\infty = 3.36$

Figure 1.- Chordwise pressure distribution on upper surface of triangular wing.

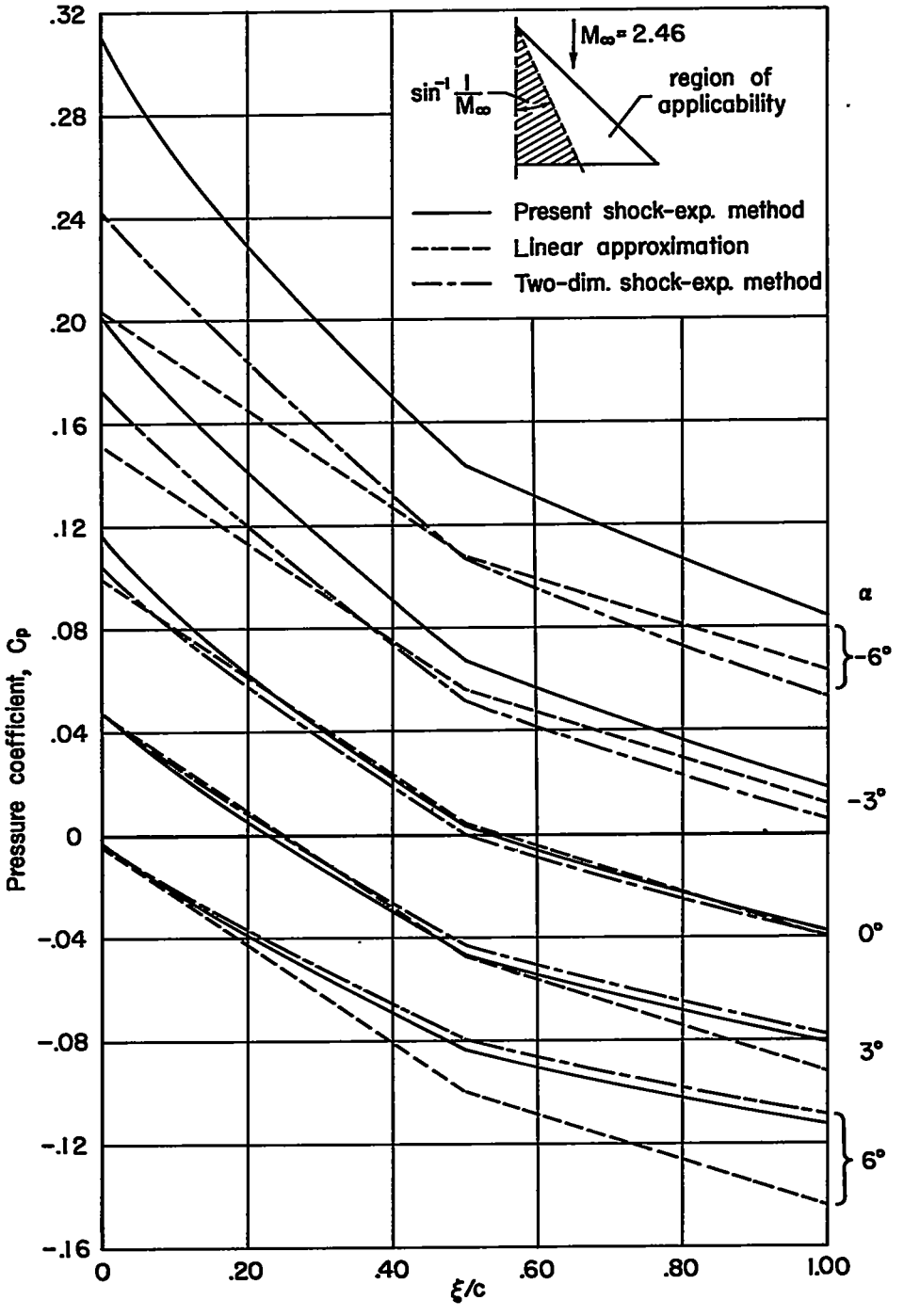

(b) $M_\infty = 2.46$

Figure 1.- Concluded.

NACA-Langley - 6-13-55 - 1000